

## LETTERS

# Linking the p53 tumour suppressor pathway to somatic cell reprogramming

Teruhisa Kawamura<sup>1,2\*</sup>, Jotaro Suzuki<sup>1,3\*</sup>, Yunyuan V. Wang<sup>1</sup>, Sergio Menendez<sup>4</sup>, Laura Batlle Morera<sup>4</sup>, Angel Raya<sup>4,5,6</sup>, Geoffrey M. Wahl<sup>1</sup> & Juan Carlos Izpisua Belmonte<sup>1,4</sup>

Reprogramming somatic cells to induced pluripotent stem (iPS) cells has been accomplished by expressing pluripotency factors and oncogenes<sup>1–8</sup>, but the low frequency and tendency to induce malignant transformation<sup>9</sup> compromise the clinical utility of this powerful approach. We address both issues by investigating the mechanisms limiting reprogramming efficiency in somatic cells. Here we show that reprogramming factors can activate the p53 (also known as Trp53 in mice, TP53 in humans) pathway. Reducing signalling to p53 by expressing a mutated version of one of its negative regulators, by deleting or knocking down p53 or its target gene, *p21* (also known as *Cdkn1a*), or by antagonizing reprogramming-induced apoptosis in mouse fibroblasts increases reprogramming efficiency. Notably, decreasing p53 protein levels enabled fibroblasts to give rise to iPS cells capable of generating germline-transmitting chimaeric mice using only Oct4 (also known as Pou5f1) and Sox2. Furthermore, silencing of p53 significantly increased the reprogramming efficiency of human somatic cells. These results provide insights into reprogramming mechanisms and suggest new routes to more efficient reprogramming while minimizing the use of oncogenes.

The p53 pathway reduces cancer initiation by inducing apoptosis or cell cycle arrest in response to a variety of stress signals, including overexpressed oncogenes such as *c-Myc*. *Klf4* can either activate or antagonize p53, depending on the cell type used and expression level<sup>10</sup>. Consequently, reprogramming efficiency is probably reduced through oncogene-mediated activation of the p53 pathway. This is consistent with previous results showing that germ cells can be spontaneously reprogrammed in the absence of p53 (ref. 11), and a combination of p53 short interfering RNA (shRNA) and *Utf1* expression increased iPS cell formation<sup>12</sup>.

We first determined whether the reprogramming factors, individually or in combination, activate the p53 pathway in mouse embryo fibroblasts (MEFs). Relative to the green fluorescent protein (GFP)-retroviral control, *c-Myc* considerably increased p53 abundance and activity, manifested by increased expression of the cyclin-dependent kinase inhibitor p21 (Fig. 1a). This was achieved by induction of p19<sup>Arf</sup>, an antagonist of Mdm2, the E3-ubiquitin ligase principally responsible for p53 degradation<sup>13</sup>. Increased p21 protein levels were also observed in MEFs infected with *Klf4* alone, with Oct4 and Sox2 (two factors) or with Oct, Sox2 and *Klf4* (three factors) (Fig. 1a). Because introducing reprogramming factors increased  $\gamma$ -H2ax (also known as  $\gamma$ -H2afx) foci (Supplementary Fig. 1), we infer that the expression of reprogramming factors may induce p53 activity by DNA damage. We also compared p53 and p21 expression in a variety of mouse and human cell lines previously used for iPS cell production

(Supplementary Fig. 2). Interestingly, keratinocytes, which have higher reprogramming efficiency, display lower p53 and p21 protein levels than other cell types. Moreover, p21 induction in keratinocytes is lower than in fibroblasts after infection with the three factors (Supplementary Fig. 3). Together, these data indicate that the p53 pathway is one determinant of reprogramming efficiency.

We therefore tested the effects of reducing p53 signalling by determining reprogramming efficiencies in cells in which p53 function was reduced by shRNA or ablated by homologous recombination. Most cells were infected with shRNA (Supplementary Fig. 4), p53 messenger RNA and protein levels were reduced by 60–80% (Fig. 1c and Supplementary Fig. 5), and iPS cell colony formation was increased by 2–4-fold using two different shRNAs (Fig. 1b, c). This probably underestimates p53 suppressive capacity, because functional p53 protein clearly remained present, as indicated by the ability of the p53 activating agent Nutlin-3a (ref. 14) to dose-dependently reduce iPS cell formation in MEFs treated with the most effective p53 shRNA (Fig. 1d). In contrast, reprogramming efficiency was increased by at least tenfold in p53-null MEFs, and this was not reduced by Nutlin-3a (Supplementary Table 1 and Fig. 1e, g). p53<sup>+/-</sup> heterozygous MEFs also exhibited higher three-factor-reprogramming efficiency than wild-type MEFs. Although culture stress can induce cellular senescence and activate p53, which would reduce reprogramming, less than 1% of the cells of all p53 genotypes stained with the senescence marker  $\beta$ -galactosidase (Supplementary Fig. 6). Because we did not detect loss of heterozygosity of the p53 gene in iPS cell colonies derived from p53<sup>+/-</sup> MEFs (Supplementary Fig. 7), the data suggest a p53 dosage-sensitivity to reprogramming (Fig. 1e). We were concerned that because p53-null MEFs are genetically unstable, increased reprogramming efficiency might result from expression of the three factors in variant cells. However, we found that re-expressing p53 protein in the p53-null MEFs markedly reduced reprogramming efficiency (Fig. 1f).

Reducing factors downstream of p53 also increased reprogramming efficiency. For example, p21 shRNA increased reprogramming by approximately threefold (Fig. 1h). This probably underestimates the magnitude to which p21 induction suppresses reprogramming as p21-shRNA-expressing cells still responded to Nutlin-3a treatment as discussed earlier. We also noted a modest induction of the pro-apoptotic factor Bax, another p53-inducible gene<sup>15</sup>, in three-factor experiments (data not shown). Consistent with a limiting role of the p53-induced apoptotic response during reprogramming, overexpression of the Bax antagonist Bcl2 suppressed apoptosis in two, three and four factor experiments, and increased the frequency of colonies expressing the pluripotency factor Nanog by fourfold

<sup>1</sup>Gene Expression Laboratory, Salk Institute for Biological Studies, 10010 North Torrey Pines Road, La Jolla, California 92037, USA. <sup>2</sup>Career-Path Promotion Unit for Young Life Scientists, Kyoto University, Kyoto 606-8501, Japan. <sup>3</sup>Drug Discovery Research, Astellas Pharma Inc., Tsukuba, Ibaraki 305-8585, Japan. <sup>4</sup>Center of Regenerative Medicine in Barcelona, Dr. Aiguader 88, 08003 Barcelona, Spain. <sup>5</sup>Institució Catalana de Recerca i Estudis Avançats (ICREA), Passeig Lluís Companys 23, 08010 Barcelona, Spain. <sup>6</sup>Networking Center of Biomedical Research in Bioengineering, Biomaterials and Nanomedicine (CIBER-BBN), Dr. Aiguader 88, 08003 Barcelona, Spain.

\*These authors contributed equally to this work.

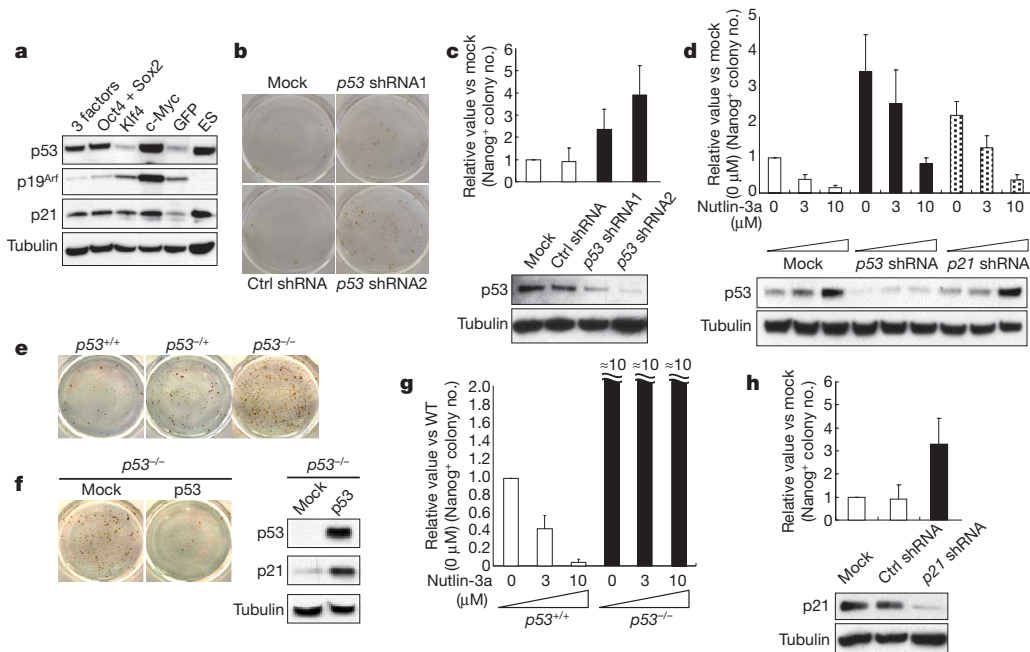


**Figure 1 | Increased generation of iPS cells by blocking p53 and p21.**

**a**, MEFs were infected by retroviruses encoding three factors (Oct4, Sox2 and Klf4), two factors (Oct4 and Sox2), Klf4, c-Myc or GFP. Four days after infection, the protein levels of p53, p19<sup>Arf</sup> and p21 were analysed by western blotting.  $\alpha$ -tubulin was used as a loading control. **b**, MEFs were infected by three factors in combination with mock, control (Ctrl) shRNA (GFP) and p53 shRNA (1 and 2). Emerging colonies of iPS cells were visualized by immunostaining with an anti-Nanog antibody using an avidin-biotin complex method. **c**, The fold-change in the number of Nanog-positive colonies compared to mock ( $n = 4$ ) (top). p53-knockdown efficiency was examined by western blot (bottom). **d**, MEFs were infected by three factors in combination with mock, p53 shRNA and p21 shRNA. Four days later, half

the cells were treated with Nutlin-3a (0, 3 and 10  $\mu$ M) and analysed for p53 levels. The remainder were stained for Nanog-positive colonies.

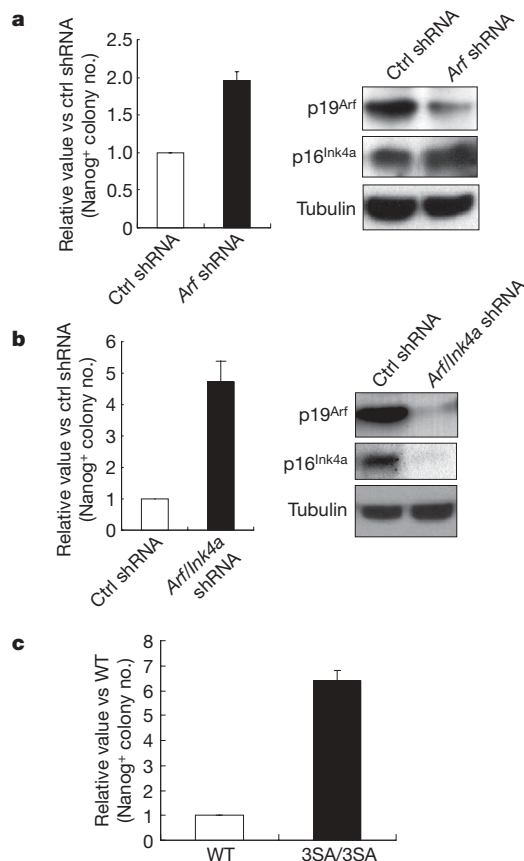
**e**, Immunostaining of Nanog-positive colonies generated from p53<sup>+/+</sup>, p53<sup>+/-</sup> and p53<sup>-/-</sup> MEFs by three-factors showed p53 dose-dependent decrease of colony number. **f**, Retroviral infection of p53 into p53<sup>-/-</sup> MEFs decreased the number of Nanog-positive colonies induced by three factors. p53 and p21 levels on day 3 after infection were analysed. **g**, Nutlin-3a markedly reduced reprogramming of p53<sup>+/+</sup> MEFs, but not of p53<sup>-/-</sup> MEFs. **h**, Fold change in the number of Nanog-positive colonies by p21 shRNA ( $n = 4$ ). p21-knockdown efficiency was examined by western blot. All error bars indicate s.d.

(Supplementary Fig. 8). The three-factor-transduced colonies exhibit the characteristics of iPS cells, with mouse embryonic stem (ES) cell morphology, high levels of alkaline phosphatase activity and expression of pluripotency-associated transcription factors and surface markers, and ability to differentiate into derivatives of all three embryonic germ layers *in vitro* (Supplementary Figs 9–11). Taken together with the genetic and shRNA studies described earlier, these data show that complete loss of p53 function markedly increases reprogramming efficiency, and that even low levels of p53 activity are all that is needed to compromise somatic cell reprogramming.

The ability of the three factors to increase p53 abundance suggests that controlling its stability might be crucial for p53-mediated reprogramming suppression. Thus we determined whether reducing p19<sup>Arf</sup> levels using *Arf* shRNA increases reprogramming efficiency, as lower *Arf* levels should decrease p53 stability<sup>16–18</sup>. Reducing p19<sup>Arf</sup> levels by 2–4-fold (Fig. 2a) engendered an approximately twofold increase in three-factor-reprogramming (Fig. 2a). Reducing p19<sup>Arf</sup> and p16<sup>Ink4a</sup> (both encoded by alternative reading frames of the *Ink4a/Arf* locus, also known as *Cdkn2a* locus) together increased iPS cell formation even more than p19<sup>Arf</sup> alone (4–5-fold; Fig. 2b), indicating that compromising retinoblastoma (Rb) tumour suppressor<sup>19</sup> function by antagonizing p16<sup>Ink4a</sup> can collaborate with diminished p53 activity to improve reprogramming efficiency.

**Figure 2 | Modulation of p53 activity alters reprogramming efficiency.**

**a**, **b**, Fold changes in the number of three-factor-induced Nanog-positive colonies by *Arf* shRNA (**a**) or by *Arf/Ink4a* shRNA (**b**) compared to control shRNA ( $n = 3$ ) (left). Protein knockdown efficiency was examined by western blot (right). **c**, Three-factor-induced Nanog-positive colonies from wild type (+/+; WT) and homozygous (3SA/3SA) MEFs ( $n = 3$ ). Error bars, s.d.



We next genetically modulated the activity of the E3 ligase that regulates p53 stability by generating a mouse encoding a mutant version of Mdmx (also known as Mdm4), a critical negative regulator of p53. We substituted three serine residues with alanines (Mdmx Ser 341, Ser 367 and Ser 402, hereafter called Mdmx3SA) to prevent its phosphorylation and degradation in response to DNA damage or activated oncogenes<sup>20,21</sup>. Notably, MEFs or thymocytes derived from homozygous Mdmx3SA mice exhibited lower basal expression of p21, lower DNA damage induced p21 levels (Supplementary Fig. 12 and ref. 21) and an impaired ability of c-Myc to activate p53 *in vivo*<sup>21</sup>. Three-factor-reprogramming increased ~7-fold in Mdmx3SA MEFs, in agreement with their reduced sensitivity to activated oncogenes and DNA damage signalling (Fig. 2c).

Because Klf4 has been reported to have oncogenic properties when overexpressed<sup>22</sup>, and we showed that it alone can activate p53, we investigated whether cells with reduced p53 expression could be converted into iPS cells using only two factors, Oct4 and Sox2. We tested this hypothesis by transducing MEFs with a lentivirus expressing p53 shRNA plus retroviruses encoding Oct4 and Sox2 (hereafter designated as 2F-p53KD-iPS cells; Supplementary Fig. 13). Cells that developed into colonies exhibiting ES-cell-like morphology were obtained by week 4 after infection. Of six colonies selected for analysis, four grew using standard mouse ES cell culturing methods (Fig. 3a), and all were alkaline-phosphatase-positive (Fig. 3b) and expressed genes and cell surface markers characteristic of mouse ES cells, including the pluripotency marker Nanog (Fig. 3c and Supplementary Fig. 14). 2F-p53KD-iPS cells and mouse ES cell lines had indistinguishable gene expression patterns when maintained under similar conditions. Bisulphite sequencing of the Oct4 and Nanog promoters showed nearly complete demethylation in 2F-p53KD-iPS cells when compared to MEFs (Supplementary Fig. 14). Consistent with this, we observed expression of the pluripotency-associated transcription factors Oct4 and Sox2 from the endogenous loci in 2F-p53KD-iPS cells, at levels that were comparable to those of ES cells (Supplementary Fig. 15).

Also, like ES cells, most (70–80%) cells were in S-phase (Supplementary Fig. 16). We tested the pluripotency of three 2F-p53KD-iPS clones in assays of embryoid body formation *in vitro* and/or teratoma induction *in vivo*. The tested cell lines differentiated into the three germ layer derivatives, as shown by immunostaining and mRNA expression *in vitro* (Fig. 3d and Supplementary Fig. 17). Furthermore, these cells differentiated with high efficiency into beating cardiomyocytes (Supplementary Fig. 18 and Supplementary Movies 1–3). After injection into immunocompromised mice, two independent 2F-p53KD-iPS lines generated complex intratesticular and subcutaneous teratomas containing structures and tissues representative of the three embryonic germ layers (Fig. 3e). Microarray analyses demonstrate that gene expression patterns of these clones are similar to mouse ES cells (Supplementary Fig. 19). We also tested whether 2F-p53KD-iPS cells contribute to the formation of chimaeric mice when injected into mouse blastocysts. One line (clone 6) contributed almost 100% to chimaera formation, and the other line (clone 1) contributed 30–50%, as judged by coat colour (Fig. 3f and Supplementary Fig. 20). We finally used the highest contribution chimaera to test for germline competence by crossing it with wild-type C57BL/6J mice. Notably, the offspring of such crosses included agouti pups (Fig. 3g), indicating germline transmission of the two-factor-iPS genome. Taken together, these results demonstrate that MEFs can be reprogrammed to pluripotency by the forced expression of only two factors, Oct4 and Sox2, when p53 levels are reduced.

We next tested whether downregulating p53 activity had any effect on the reprogramming of human embryonic fibroblasts (HEFs) and juvenile epidermal keratinocytes. We could not obtain Nanog-positive colonies from HEFs with either three or four factors combined with control shRNA under our reprogramming conditions after up to 4 weeks. In contrast, cell reprogramming occurred rapidly (after 2 weeks) with high efficiency when p53 expression was reduced by shRNA (Fig. 4a and Supplementary Figs 22, 23 and Supplementary Table 2). p53 shRNA induced ES-cell-like colonies, expressed human

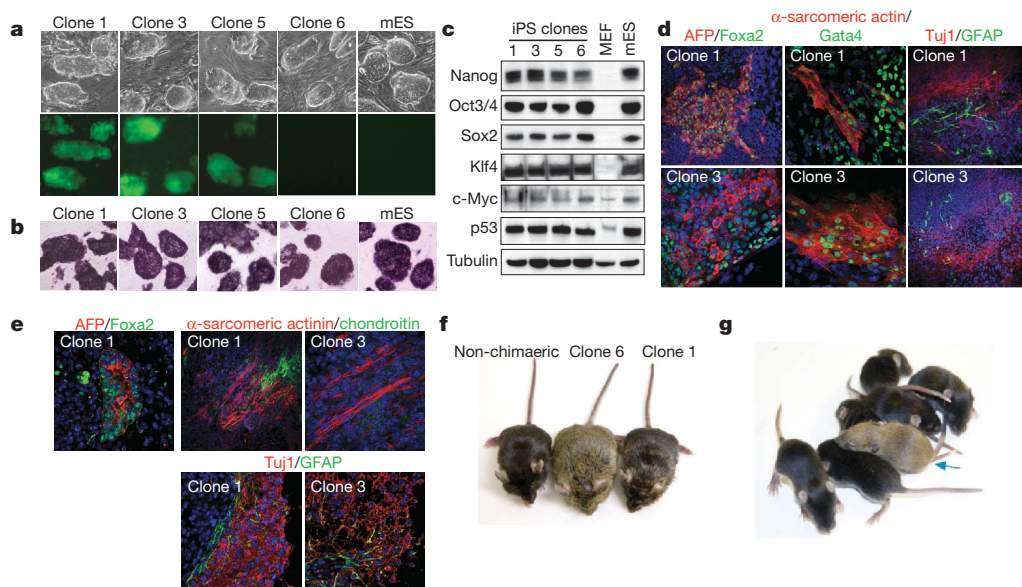


**Figure 3 | Generation and characterization of 2F-p53KD-iPS cells by p53 downregulation.** **a**, Morphology and GFP fluorescence of 2F-p53KD-iPS cell lines. GFP expression is silenced in clone 6. mES, mouse ES cells. **b**, Alkaline phosphatase staining of 2F-p53KD-iPS cell lines. DAPI (4,6-diamidino-2-phenylindole) was used to visualize cell nuclei. Original magnification (**a**, **b**),  $\times 200$ . **c**, Protein levels of Nanog, Oct4, Sox2, Klf4, c-Myc and p53 in 2F-p53KD-iPS cell lines are shown.  $\alpha$ -tubulin was used as loading control. **d**, Embryoid bodies of 2F-p53KD-iPS cell clones on day 6 of differentiation. Embryoid bodies were transferred to gelatinized dishes on days 3 to 5 for further differentiation. On day 14, embryoid bodies were subjected to immunofluorescence for  $\alpha$ -fetoprotein (AFP) and Foxa2 (endoderm),

$\alpha$ -sarcomeric actin and Gata4 (mesoderm) and Tuj1 and GFAP (ectoderm). **e**, Immunofluorescence of teratoma from 2F-p53KD-iPS cells using antibodies against AFP and Foxa2 (endoderm), sarcomeric  $\alpha$ -actinin and chondroitin (mesoderm), and Tuj1 and GFAP (ectoderm) showed spontaneous differentiation into all three germ layers. Original magnification (**d**, **e**),  $\times 400$ . **f**, Adult chimaeric mice obtained from 2F-p53KD-iPS cell lines (1 and 6) and non-chimaeric mouse in C57BL/6J host blastocysts. **g**, As of the date of submission, the mating of offspring from clone 6 chimaera to a C57BL/6J female generated 1 agouti pup (blue arrow), that together with PCR analysis (not shown) indicate germline transmission of the two-factor iPS genome.

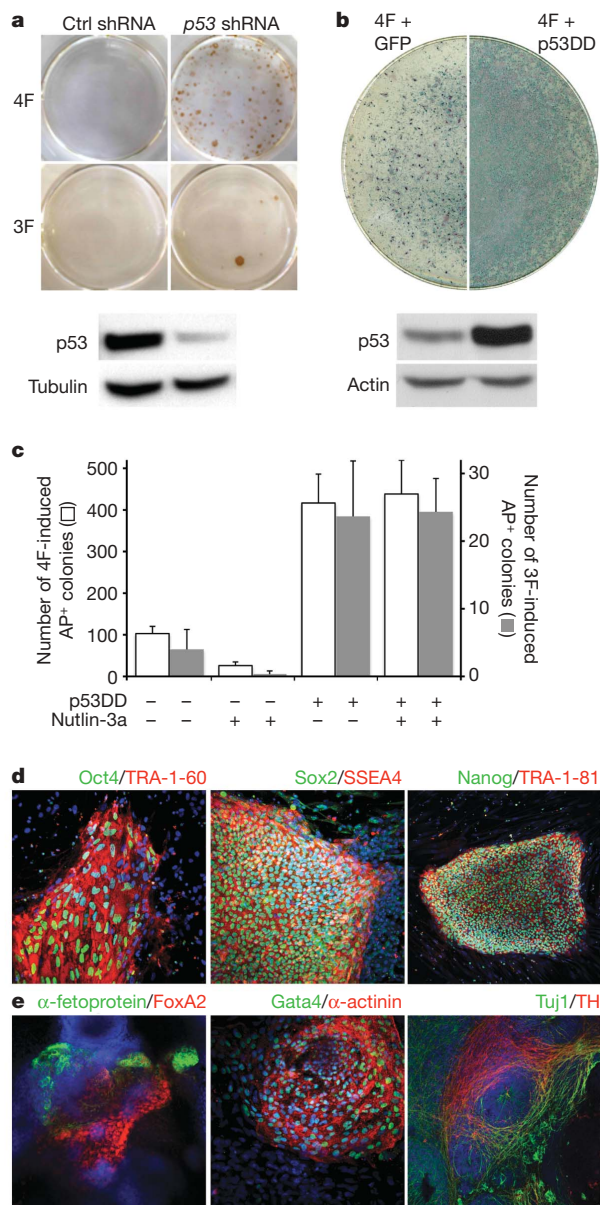


**Figure 4 | Downregulation of p53 activity increases reprogramming efficiency of human somatic cells.** **a**, HEFs were infected with retroviruses encoding Oct4, Sox2 and Klf4 (three factors, or 3F) or Oct4, Sox2, Klf4 and c-Myc (four factors, or 4F) in combination with lentiviruses expressing control or p53 shRNA. Emerging colonies of iPS cells were immunostained with anti-Nanog antibody (top). p53-knockdown efficiency was examined by western blot (bottom). **b**, Human primary keratinocytes were co-infected with four factors and retroviruses expressing GFP or p53DD. After 2 weeks, cells were stained for alkaline phosphatase activity (top). Expression of p53DD resulted in stabilization of wild-type p53 (bottom). Actin was used as a loading control. **c**, The average number of iPS-cell-like colonies obtained from  $10^4$  keratinocytes reprogrammed with three or four factors and retroviruses encoding GFP or p53DD, in the absence or presence of Nutlin-3a ( $n = 3$ ). iPS-cell-like colonies were scored as having human ES-cell-like morphology and positive alkaline phosphatase staining. Owing to the numerous colonies generated in four-factor p53DD keratinocytes, quantification was done using  $10^4$  cells. Error bars, s.d. **d, e**, Colonies of human keratinocyte-derived iPS cells generated by three factors and p53DD show strong immunoreactivity for pluripotency-associated transcription factors (Oct4, Sox2, and Nanog) and surface markers (TRA-1-60 and TRA-1-81) (**d**) and differentiate *in vitro* into cell types that express markers of endoderm ( $\alpha$ -fetoprotein, FoxA2), mesoderm (Gata4, sarcomeric  $\alpha$ -actinin), and ectoderm (Tuj1, tyrosine hydroxylase (TH)) (**e**).

ES cell marker genes, could be successfully cloned and expanded, exhibited ES-cell-like morphology, and differentiated *in vitro* in embryoid body formation assays (Supplementary Figs 24 and 25). We also obtained two-factor-induced iPS cell colonies from HEFs infected with p53 shRNA, although with lower efficiency (two iPS cell colonies resulted from six independent attempts, Supplementary Fig. 26). Consistently, reprogramming efficiency was increased using either three or four factors in human primary keratinocytes when p53 activity was downregulated using a dominant negative mutant of p53 (p53DD)<sup>23</sup> (Fig. 4b, c) that inhibited p53 activity more effectively than p53 shRNA, because Nutlin-3a did not reduce reprogramming of three-factor or four-factor p53DD expressing iPS cells (Fig. 4c). 3F-p53DD-iPS cells grew robustly and strongly expressed pluripotency-associated transcription factors and surface markers (Fig. 4d and data not shown). Furthermore, 3F-p53DD-iPS cells readily differentiated *in vitro* into derivatives of the three embryonic germ layers as judged by cell morphology and specific immunostaining (Fig. 4e). These results show that p53 activity limits reprogramming of both mouse and human cells.

Oct4, Sox2 and Nanog interact with each other to enable the genome-wide chromatin remodelling required for induction of pluripotency. None of these factors are expressed at detectable levels in somatic cells. Previous work showed that p53 represses Nanog in response to DNA damage in ES cells<sup>24</sup>, raising the possibility that p53 might prevent Nanog expression in MEFs. However, we observed that *Nanog* mRNA was not expressed at detectable levels in either p53 wild-type or p53-null MEFs (Supplementary Fig. 11a and data not shown). On the other hand, the oncogene *Klf4* has been reported to induce *Nanog*<sup>25</sup>. It is possible that in the absence of *Klf4* in two-factor iPS cells, p53 elimination allowed Oct4 and Sox2 to remodel the chromatin to a threshold required for expression of sufficient *Nanog* to drive the subsequent events involved in iPS cell generation.

Our data show that reprogramming somatic cells to iPS cells is associated with activation of the p53 pathway, which acts as a barrier to reprogramming. The mechanisms by which p53 antagonizes reprogramming seem to involve both its ability to limit cell cycling by induction of the cyclin-dependent kinase inhibitor p21 and its ability to induce apoptosis. This suggests that direct chemical inhibition of the apoptotic cascade may provide a useful tool for enhancing reprogramming efficiency without direct genetic manipulation of tumour suppressors. We also show that reprogramming in the absence of oncogenes such as c-Myc and Klf4 will require inactivating the p53 and Rb tumour suppressors. Although p53 pathway inactivation will be key, this cannot be done on a permanent basis, as this would increase the probability of malignant transformation and the generation of unstable genomes that would mitigate their use for understanding many diseases. Rather, transient inhibition using chemical antagonists or reversible approaches that avoid genetic disruption will be required<sup>12,26</sup>. As Oct4 and Sox2 are oncogenic when overexpressed, using small molecules or proteins to transiently mimic their reprogramming functions<sup>27–29</sup> may enable oncogene-free iPS cells to be obtained at acceptable frequencies. The mechanistic insights we provide (Supplementary Fig. 27) should shorten the road to developing clinically useful iPS cells.

## METHODS SUMMARY

MEFs were isolated from embryonic day (E) 13.5 embryos obtained from wild-type, p53-deficient, or Mdmx-mutant mice. Retroviral and lentiviral viruses were produced in HEK293 cells, and 12 to 14 days after infection MEFs were fixed for immunofluorescence. Reprogramming of HEFs (IMR90) and keratinocytes was done as previously described<sup>2,3,6</sup>. Around two to three weeks after infection, cells were fixed for immunofluorescence studies. As for two-factor iPS cell formation, after a minimum of 4 weeks, colonies derived from infected MEFs or IMR90 cells were fixed for immunostaining or picked up for clonal expansion. Protein, mRNA, promoter methylation, microarray and immunofluorescence analyses were performed by standard methods<sup>30</sup>. *In vitro* differentiation of mouse iPS cells was established by the hanging-drop method, whereas human iPS cells were differentiated by suspension culture. Teratomas were induced by

injecting iPS cells subcutaneously and into the testicles, and analysed three to four weeks after injection. Chimaeric mice were obtained by injecting iPS cells into C57BL/6J hosts. High-contribution chimaeras were mated to C57BL/6J mice to test for germline transmission.

**Full Methods** and any associated references are available in the online version of the paper at [www.nature.com/nature](http://www.nature.com/nature).

Received 6 March; accepted 23 July 2009.

Published online 9 August 2009.

1. Takahashi, K. & Yamanaka, S. Induction of pluripotent stem cells from mouse embryonic and adult fibroblast cultures by defined factors. *Cell* **126**, 663–676 (2006).
2. Takahashi, K. *et al.* Induction of pluripotent stem cells from adult human fibroblasts by defined factors. *Cell* **131**, 861–872 (2007).
3. Yu, J. *et al.* Induced pluripotent stem cell lines derived from human somatic cells. *Science* **318**, 1917–1920 (2007).
4. Park, I. H. *et al.* Reprogramming of human somatic cells to pluripotency with defined factors. *Nature* **451**, 141–146 (2008).
5. Lowry, W. E. *et al.* Generation of human induced pluripotent stem cells from dermal fibroblasts. *Proc. Natl Acad. Sci. USA* **105**, 2883–2888 (2008).
6. Aasen, T. *et al.* Efficient and rapid generation of induced pluripotent stem cells from human keratinocytes. *Nature Biotechnol.* **26**, 1276–1284 (2008).
7. Nakagawa, M. *et al.* Generation of induced pluripotent stem cells without Myc from mouse and human fibroblasts. *Nature Biotechnol.* **26**, 101–106 (2008).
8. Wernig, M., Meissner, A., Cassady, J. P. & Jaenisch, R. c-Myc is dispensable for direct reprogramming of mouse fibroblasts. *Cell Stem Cell* **2**, 10–12 (2008).
9. Okita, K., Ichisaka, T. & Yamanaka, S. Generation of germline-competent induced pluripotent stem cells. *Nature* **448**, 313–317 (2007).
10. Rowland, B. D., Bernards, R. & Peepker, D. S. The KLF4 tumour suppressor is a transcriptional repressor of p53 that acts as a context-dependent oncogene. *Nature Cell Biol.* **7**, 1074–1082 (2005).
11. Kanatsu-Shinohara, M. *et al.* Generation of pluripotent stem cells from neonatal mouse testis. *Cell* **119**, 1001–1012 (2004).
12. Zhao, Y. *et al.* Two supporting factors greatly improve the efficiency of human iPSC generation. *Cell Stem Cell* **3**, 475–479 (2008).
13. Cleveland, J. L. & Sherr, C. J. Antagonism of Myc functions by Arf. *Cancer Cell* **6**, 309–311 (2004).
14. Vassilev, L. T. *et al.* *In vivo* activation of the p53 pathway by small-molecule antagonists of MDM2. *Science* **303**, 844–848 (2004).
15. Miyashita, T. & Reed, J. C. Tumor suppressor p53 is a direct transcriptional activator of the human *bax* gene. *Cell* **80**, 293–299 (1995).
16. Kamijo, T. *et al.* Functional and physical interactions of the ARF tumor suppressor with p53 and Mdm2. *Proc. Natl Acad. Sci. USA* **95**, 8292–8297 (1998).
17. Pomerantz, J. *et al.* The *Ink4a* tumor suppressor gene product, p19<sup>Arf</sup>, interacts with MDM2 and neutralizes MDM2's inhibition of p53. *Cell* **92**, 713–723 (1998).
18. Zhang, Y., Xiong, Y. & Yarbrough, W. G. ARF promotes MDM2 degradation and stabilizes p53: ARF-*INK4a* locus deletion impairs both the Rb and p53 tumor suppression pathways. *Cell* **92**, 725–734 (1998).
19. Knudsen, E. S. & Knudsen, K. E. Tailoring to RB: tumour suppressor status and therapeutic response. *Nature Rev. Cancer* **8**, 714–724 (2008).
20. Marine, J. C., Dyer, M. A. & Jochemsen, A. G. MDMX: from bench to bedside. *J. Cell Sci.* **120**, 371–378 (2007).
21. Wang, Y. V. *et al.* Increased radioresistance and accelerated B cell lymphomas in mice with Mdmx mutations that prevent modifications by DNA-damage-activated kinases. *Cancer Cell* **16**, 33–43 (2009).
22. Foster, K. W. *et al.* Oncogene expression cloning by retroviral transduction of adenovirus E1A-immortalized rat kidney RK3E cells: transformation of a host with epithelial features by c-MYC and the zinc finger protein GKLf. *Cell Growth Differ.* **10**, 423–434 (1999).
23. Shaulian, E., Zauberman, A., Ginsberg, D. & Oren, M. Identification of a minimal transforming domain of p53: negative dominance through abrogation of sequence-specific DNA binding. *Mol. Cell. Biol.* **12**, 5581–5592 (1992).
24. Lin, T. *et al.* p53 induces differentiation of mouse embryonic stem cells by suppressing *Nanog* expression. *Nature Cell Biol.* **7**, 165–171 (2005).
25. Jiang, J. *et al.* A core Klf circuitry regulates self-renewal of embryonic stem cells. *Nature Cell Biol.* **10**, 353–360 (2008).
26. Komarov, P. G. *et al.* A chemical inhibitor of p53 that protects mice from the side effects of cancer therapy. *Science* **285**, 1733–1737 (1999).
27. Shi, Y. *et al.* Induction of pluripotent stem cells from mouse embryonic fibroblasts by Oct4 and Klf4 with small-molecule compounds. *Cell Stem Cell* **3**, 568–574 (2008).
28. Huangfu, D. *et al.* Induction of pluripotent stem cells from primary human fibroblasts with only Oct4 and Sox2. *Nature Biotechnol.* **26**, 1269–1275 (2008).
29. Kim, D. *et al.* Generation of human induced pluripotent stem cells by direct delivery of reprogramming proteins. *Cell Stem Cell* **4**, 472–476 (2009).
30. Gonzalez, F. *et al.* Generation of mouse-induced pluripotent stem cells by transient expression of a single nonviral polycistronic vector. *Proc. Natl Acad. Sci. USA* **106**, 8918–8922 (2009).

**Supplementary Information** is linked to the online version of the paper at [www.nature.com/nature](http://www.nature.com/nature).

**Acknowledgements** We are grateful to the CMRB Histology & Bioimaging and Cell culture Platforms for assistance, S. Boue for microarray analysis, S. Kim for help with maintenance of mouse colonies, Y. Richaud for technical assistance, M. Nagao for preparation of mouse neural stem cells, K. Brennand and F. Gage for preparation of human neural stem cells, I. Verma and A. Consiglio for advice and help with lentiviral transduction, Y. Dayn for chimaeric mouse production, and all members of the Gene Expression Laboratory and CMRB for discussions and M. Serrano for sharing unpublished results. J.S. was partially supported by Astellas Pharma Inc. T.K. was partially supported by Japan Society for the Promotion of Science. Work in the laboratory of G.M.W. was supported by NIH grants (5 R01 CA061449 and CA100845). Work in the laboratory of J.C.I.B. was supported by grants from the NIH, Tercel, Marato, G. Harold and Leila Y. Mathers Charitable Foundation and Fundacion Cellex.

**Author Contributions** T.K. and J.S. contributed to the experimental work, project planning, data analysis and writing the manuscript and contributed equally to this work. Y.V.W. contributed to the experimental work, data analysis, writing the manuscript and established Mdmx mutant mice. S.M., L.B.M. and A.R. contributed to the experimental work, data analysis and writing the manuscript. G.M.W. and J.C.I.B. contributed to project planning and writing the manuscript, and supervised all the work. G.M.W. and J.C.I.B. are co-contributing corresponding authors.

**Author Information** Reprints and permissions information is available at [www.nature.com/reprints](http://www.nature.com/reprints). Correspondence and requests for materials should be addressed to J.C.I.B. ([belmonte@salk.edu](mailto:belmonte@salk.edu)) or G.M.W. ([wahl@salk.edu](mailto:wahl@salk.edu)).

## METHODS

**Reagents.** Reagents were obtained from the following sources: Nutlin-3a (Cayman Chemical); anti-Oct-3/4 (sc-5279), anti-GKLF (sc-20691), anti-p53 (sc-6243), anti-p21 (sc-53870), anti-p16<sup>Ink4a</sup> (sc-1207), anti-c-Myc (sc-764) and anti-Gata4 (sc-9053) (Santa Cruz Biotechnology); anti-Sox2 (AB5603) (Chemicon); anti-p53 antibody (1C12), anti-phospho-Histone H2A.X (Ser139) antibody (20E3) (Cell Signaling); anti-p19<sup>Arf</sup> (ab80) and anti-Nanog (ab21603) (Abcam); anti-Nanog (SC1000) and anti-p53 (DO-1) (Calbiochem); anti-Tuj1 antibody (MMS-435P-0) (Covance); anti- $\alpha$ -tubulin (T5168), anti- $\alpha$ -actinin sarcomeric (A7811), anti- $\alpha$ -actin sarcomeric (A2172), anti-actin (A2066) and anti-chondroitin (C8035) (Sigma); anti-Foxa2 antibody (AF2400) (R&D systems); anti-alpha-1-fetoprotein (A008) and anti-GFAP (Z0334) (Dako); anti-TRA-1-81 antibody (Millipore).

**Mice.** Wild-type MEFs used for iPS cell production were derived from embryos obtained by mating BDF1/ICR and ICR strains. *p53*-knockout mice were purchased from Taconic Farms, Inc. *p53*<sup>-/-</sup> MEFs were obtained by heterozygous versus heterozygous mating. For genotyping, PCR primers are available on the company website. *Mdmx*-mutant mice were generated from ES cells of 129Sv origin by homologous recombination<sup>21</sup>.

**Plasmids.** Mouse *p53* and GFP complementary DNAs were cloned into pMXs retroviral vectors<sup>31</sup>. The cDNA of mouse *Bcl2* was cloned into HIV pBOBI lentiviral vector<sup>32</sup>. Human p53DD (a gift from M. Oren) is in pLXSN (Clontech). The cDNAs of mouse *p53* and *p21*, pMXs-Oct4, -Sox2, -Klf4 and -c-Myc were purchased from Addgene<sup>1,33,34</sup>. Human pMSCV-Oct4, -Sox2, -Klf4 and -c-Myc were constructed as previously described<sup>6</sup>. The shRNA sequences against *p53*, *p21*, *Arf* and *Ink4a* were inserted into pLVTHM lentiviral vectors<sup>36</sup>. Sequences for shRNA are shown in Supplementary Table 3.

**Production of retroviruses and lentiviruses and iPS cell formation.** VSV-G viruses were produced in HEK293T cells. For pMX-based and pMSCV-based retroviruses, vectors were transfected using CaPO<sub>4</sub> or lipofectamine, following the manufacturers' directions. One day after transfection, culture medium was changed to new medium. For lentivirus, pBOBI-based<sup>32</sup> or pLVTHM-based<sup>36</sup> vectors were transfected by Lipofectamine 2000 (Invitrogen) according to the manufacturer's protocol. Six hours after transfection, the DNA-lipofectamine-complex was removed and the medium was replaced the next day. Two days after transfection, the supernatant containing viruses was collected and filtered through a 0.45- $\mu$ m filter. Mouse iPS cells were induced as previously described<sup>35,37</sup>. In brief, MEFs (passage 3–5) were infected (day 0) with pMX-based retroviruses together with pLVTHM-based lentivirus for shRNAs or pBOBI-based lentivirus for *Bcl2*. On day 2, cells were passed onto new gelatin-coated plates. Medium was changed every 2 days. On days 12 to 14, cells were fixed for immunofluorescence study. For the Nutlin-3a experiments, cells were treated starting from day 4. Reprogramming of HEFs (IMR90) was done as previously described<sup>2,3</sup>. In brief, IMR90 fibroblasts (passage 7–9) were infected (day 0) with pMSCV-based retroviruses plus pLVTHM-based lentiviruses for *p53* shRNA. On day 4 or 5, cells were passed onto feeder MEFs. Medium was changed every other day. Around 3 weeks after infection, cells were fixed for immunofluorescence studies. Reprogramming of human primary keratinocytes was carried out essentially as described<sup>6</sup>. Cells were co-infected with retroviral supernatants containing 3 or 4 reprogramming factors and p53DD or GFP at a 1:2 ratio. To assess the reprogramming efficiency, cells were trypsinized 3 days after retroviral infection and 10<sup>4</sup> cells were plated onto 6-cm tissue culture dishes on top of irradiated human foreskin fibroblasts with human ES cell medium. After 2 weeks, the dishes were stained for alkaline phosphatase activity and colonies that displayed strong staining and showed human ES-cell-like

morphology were scored positive. As for two-factor iPS cell formation, MEFs or IMR90 cells were co-infected with retroviral supernatants containing two factors (Oct4 and Sox2) and lentivirus supernatants (*p53* shRNA) at a 1:1:3 ratio. Infected cells were passed onto new gelatin-coated plates at day 2 (MEFs) or onto feeder MEFs at day 5 (IMR90). Medium was changed every other day, and after a minimum of 4 weeks, colonies were fixed for immunostaining or picked up for clonal expansion.

**Protein and mRNA analysis.** Cells were washed once in PBS and lysed in 2 $\times$  SDS-PAGE sample buffer without 2-mercaptoethanol and glycerol. Lysates were briefly sonicated and cleared by centrifugation. The protein concentration was determined by a BCA Protein Assay Kit (Thermo Scientific). Lysates were then mixed with 2-mercaptoethanol, bromophenol blue and glycerol, and boiled. Equal amounts of proteins were subjected to SDS-PAGE. Total RNA was isolated using Trizol (Invitrogen) followed by cDNA synthesis using Superscript II Reverse Transcriptase (Invitrogen). Quantitative PCR was performed using SYBR Green PCR Master Mix (Applied Biosystems). Primer sequences are available on request.

**Promoter methylation analysis.** Genomic DNA was isolated and bisulphite modification performed using the EZ DNA Methylation-Direct Kit (Zymo Research). The promoter regions of *Nanog* and *Oct4* were amplified by nested PCR using primer sets previously described<sup>38</sup>. The amplified PCR products were ligated into pCRII-TOPO (Invitrogen) and sequenced. Data was analysed using Lasergene (Dnastar).

**In vitro and in vivo differentiation.** For *in vitro* differentiation of mouse iPS cells, after dissociation with trypsin/EDTA, cells were cultured in suspension by the hanging-drop method. For *in vivo* differentiation, cells were trypsinized, and injected subcutaneously into severe combined immunodeficient (SCID) mice. After 3 weeks, teratomas were dissected, fixed and analysed. Detailed methods for *in vitro* differentiation, teratoma formation and immunostaining are described in Supplementary Methods. *In vitro* differentiation of HEF-derived human iPS cells was induced by culturing cells in suspension and then transferring onto gelatine-coated dishes. *In vitro* differentiation of keratinocytes-derived human iPS cells was carried out as previously described<sup>6</sup>.

**Blastocyst injections for chimaeric mice.** iPS cells were injected into C57BL/6J hosts blastocysts and transferred into 2.5 days post-coitum ICR pseudopregnant recipient females. Chimaerism was ascertained after birth by the appearance of agouti coat colour (from iPS cells) in black host pups. High-contribution chimaeras were mated to C57BL/6J mice to test for germline transmission.

- Kitamura, T. *et al.* Retrovirus-mediated gene transfer and expression cloning: powerful tools in functional genomics. *Exp. Hematol.* **31**, 1007–1014 (2003).
- Miyoshi, H., Blömer, U., Takahashi, M., Gage, F. H. & Verma, I. M. Development of a self-inactivating lentivirus vector. *J. Virol.* **72**, 8150–8157 (1998).
- Sherley, J. L. Guanine nucleotide biosynthesis is regulated by the cellular p53 concentration. *J. Biol. Chem.* **266**, 24815–24828 (1991).
- Huppi, K. *et al.* Molecular cloning, sequencing, chromosomal localization and expression of mouse p21 (*Waf1*). *Oncogene* **9**, 3017–3020 (1994).
- Takahashi, K., Okita, K., Nakagawa, M. & Yamanaka, S. Induction of pluripotent stem cells from fibroblast cultures. *Nature Protocols* **2**, 3081–3089 (2007).
- Wiznerowicz, M. & Trono, D. Conditional suppression of cellular genes: lentivirus vector-mediated drug-inducible RNA interference. *J. Virol.* **77**, 8957–8961 (2003).
- Blelloch, R., Venere, M., Yen, J. & Ramalho-Santos, M. Generation of induced pluripotent stem cells in the absence of drug selection. *Cell Stem Cell* **1**, 245–247 (2007).
- Blelloch, R. *et al.* Reprogramming efficiency following somatic cell nuclear transfer is influenced by the differentiation and methylation state of the donor nucleus. *Stem Cells* **24**, 2007–2013 (2006).